

Published in final edited form as:

J Orthop Res. 2012 April ; 30(4): 547–553. doi:10.1002/jor.21548.

Selective inhibition of the MCP-1-CCR2 ligand-receptor axis decreases systemic trafficking of macrophages in the presence of UHMWPE particles

Emmanuel Gibon^{1,2}, Ting Ma¹, Pei-Gen Ren¹, Kate Fritton¹, Sandip Biswal³, Zhenyu Yao¹, Lane Smith¹, and Stuart B. Goodman¹

¹Department of Orthopaedic Surgery, Stanford University School of Medicine, Stanford California

²Department of Orthopaedic Surgery, Bichat Teaching Hospital, Paris School of Medicine, Paris VII University, Paris, France

³Department of Radiology, Stanford University School of Medicine, Stanford California

Abstract

The biological mechanisms leading to periprosthetic osteolysis involve both chemokines and the monocyte/macrophage cell lineage. Whether MCP-1 plays a major role in macrophage recruitment in the presence of wear particles is unknown. We tested two hypotheses: (1) that exogenous local delivery of MCP-1 induces systematic macrophage recruitment and (2) that blockade of the MCP-1 ligand-receptor axis decreases macrophage recruitment and osteolysis in the presence of UHMWPE particles. Six groups of nude mice were used. We used non-invasive imaging to assay macrophage recruitment and osteolysis. A murine macrophage cell line and primary wild type and CCR2 knockout murine macrophages were used as the reporter cells. Particles were infused into the femoral canal. Bioluminescence and immunohistochemical staining were used to confirm the migration of reporter cells. Locally infused MCP-1 induced systemic macrophage trafficking to bone. Injection of MCP-1 receptor antagonist significantly decreased reporter cell recruitment to bone infused with UHMWPE particles and decreased osteolysis. Systemic migration of reporter cells to infused particles was decreased when the reporter cells were deficient in the CCR2 receptor. Interruption of the MCP-1 ligand-receptor axis appears to be a viable strategy to mitigate trafficking of macrophages and osteolysis due to UHMWPE particles.

Keywords

Arthroplasty; UHMWPE particles; macrophage recruitment; MCP-1; osteolysis

Introduction

Aseptic loosening remains one of the most common causes of failure of joint arthroplasties. Sundfeldt et al.¹ showed that this etiology accounts for up to two-thirds of hip revisions and one half of knee revisions. The number of total hip arthroplasty (THA) and total knee arthroplasty (TKA) revisions will increase 137% and 601%, respectively, over the next 25 years.² Therefore, increasing the lifetime of joint replacements is a current challenge.

Aseptic loosening has a multifactorial etiology including physical and biological factors.¹ Macrophages are widely represented among cell populations found in retrieval studies³⁻⁶ and act as a key cell in the inflammatory response to wear particles. Wear particles can be found in the joint, and along the interface between the prosthesis and bone.⁷ Given that most particles are submicron in size⁸ and that macrophages can increase bone resorption activity in the presence of wear debris, osteolysis is relevant to the survivorship of joint replacements.⁹

Production of ultra high molecular weight polyethylene (UHMWPE) particles leads to a non-specific macrophage-mediated foreign body immune reaction¹⁰ that can lead to high local levels of pro-inflammatory cytokines and chemokines. Moreover, UHMWPE particles induce systemic macrophage recruitment¹¹⁻¹³ and pro-inflammatory cytokine release¹⁴ resulting in osteolysis.^{15,16} Once phagocytosis of UHMWPE particles occurs, macrophages release pro-inflammatory cytokines through NF- κ B activation via several intracellular signal transduction pathways, inducing a series of biological events such as recruitment of more macrophages and osteoclast precursors, their differentiation¹⁷, and further release of cytokines and chemokines.¹⁸ Monocyte chemoattractant protein-1 (MCP-1/CCL2/MCAF/TDCF) is one of the most abundantly released chemokines¹⁹ and is an immediate early stress-responsive factor.²⁰ MCP-1 acts through its receptor CCR2, which exists in two isoforms (CCR2A and CCR2B). Deshamane et al. showed that the CCR2B isoform is predominantly expressed by monocytes and activated NK cells.²¹ MCP-1 is also released by fibroblasts and bone marrow derived primary osteoblasts in the presence of wear debris²² and requires G-protein activation.²³ Previous studies demonstrated a relationship between macrophage exposure to wear particles and MCP-1 expression,^{14,24-32} but the role of MCP-1 in local and systemic trafficking of inflammatory cells in the presence of UHMWPE particles remains unknown. We hypothesized that wear particle-induced macrophage recruitment and bone loss can be mitigated by interruption of the MCP-1-CCR2 ligand-receptor axis. In this study, we test this hypothesis using a murine model of continuous intramedullary infusion of clinically relevant UHMWPE particles.

MATERIALS AND METHODS

Animals and experimental design

56 8 to 9 wk-old nude mice nu/nu (Charles River Laboratory Inc, Wilmington, MA) were housed and fed in our Animal Facility. The experimental design was approved by the Institutional Administration Panel for Laboratory Animal Care (APLAC number 9037). Animals were divided into 6 groups (Table. 1). Group 1 had UHMWPE particles infused into the distal femur via a minipump; animals were also injected intraperitoneally with 0.1 mL of RS102895 (a soluble competitive CCR2B receptor inhibitor, Sigma-Aldrich, St-Louis, MO) twice a week at a concentration of 5mg/ml. Group 2 had infused UHMWPE particles; the animals were also injected intraperitoneally twice a week with 0.1 mL of the carrier solution: 40 μ l DMSO (Sigma-Aldrich) in 960 μ l PBS (Sigma-Aldrich). For Groups 1 and 2, the reporter cells injected via the tail vein were the macrophage cell line RAW264.7. Groups 3 and 4 had infused particles and were injected via the tail vein with either CCR2 $-/-$ or wild type reporter macrophages. Group 5 had a single injection of sterile saline solution into the femoral marrow space. Group 6 had a single injection of MCP-1 into the marrow space to confirm localization of migrated reporter macrophages induced by MCP-1. For Groups 5 and 6, tail vein injections were performed with the macrophage cell line RAW264.7.

For Groups 1 and 2, RS102895 (an antagonist of CCR2B receptor) and the carrier solution were injected during 5 wks (2 wks before surgery and 3 wks after). All groups were injected intravenously with reporter cells (day 0) 1 wk after surgery, when wound healing was

complete. Groups 1 and 2 underwent a microCT 1 day before surgery and at day 20 for bone mineral density analysis. Bioluminescence (BLI) was performed at day 0, 2, 4, 6, 8, 10, 14, and 19 for Groups 1 and 2 and at day 0, 2, 3, 4, 7, 9 for Groups 5 and 6. All animals were euthanized after imaging, and their femurs were harvested for histomorphometry.

Surgery

Surgery was performed at day 7 (7 days before imaging began). All animals received an injection of buprenorphine (0.1 mg/kg; Ben Venue Labs., Bedford, OH), subcutaneously before the procedure. Animals were anesthetized with 3% isoflurane in 100% oxygen at a flow rate of 1 L/min and were operated on a warm small animal surgery station. The left patellar tendon was exposed through a 5 mm skin incision. Then the intercondylar notch of the distal femur was exposed through a medial parapatellar arthrotomy. We used a series of needles (25 to 21 gauge) to manually drill through the intercondylar notch. To implant the osmotic pump subcutaneously, another incision was made posteriorly between the scapulae. Then we filled the femoral shaft with UHMWPE particles and a 23 gauge hollow, 6-mm long rod, connected to the pump via polyvinyl tubing was press fit into the distal femur through the drill hole (Fig. 1A). After implant insertion, the quad-patellar complex was closed by one 6.0 chromic-gut resorbable suture and the skin (knee and dorsal incisions) was repaired with 5.0 vicryl sutures and biocompatible glue. Animals were checked each day post-op for general health and activity.

Particles and pumps

We used conventional non-highly cross-linked UHMWPE particles (a gift from Dr. Timothy Wright) obtained from knee joint simulator tests and isolated according to an established protocol.³³ The particles were isolated by density gradient centrifugation and sterilized by incubating with 95% ethanol overnight. Then frozen aliquots of the particles containing serum were lyophilized for 4 to 7 days. The dried material was digested in 5M sodium hydroxide at 70°C for 2 hrs. The digested particle suspension was centrifuged through a 5% sucrose gradient at 40 K rpm at 10°C for 3 hrs. The collected particles at the surface of the sucrose solution were ultrasonicated and centrifuged again through an isopropanol gradient (0.96 and 0.90 g/cm³) at 40 K rpm at 10°C for 1 hr. The purified particles at the interface between the two layers of isopropanol were harvested and the isopropanol was evaporated from the particle mixture until dry. Particles were then resuspended in 95% ethanol that was evaporated completely. Ultimately, UHMWPE particles were washed in 70% ethanol and resuspended in PBS prior to filling the micropumps. The particle concentration was 15mg/mL. The particles tested negative for endotoxin using a Limulus Amebocyte Lysate Kit (Bio Whittaker, Walkersville, MD). The mean particle diameter was $1.0 \pm 0.1 \mu\text{m}$ (mean \pm SE) measured by electron microscopy (Fig. 2). We used a Model 2006 Alzet osmotic pump (DURECT Corp, Cupertino, CA) loaded with the particles connected to silicon tubing overlying a 6 mm long hollow Ti rod. 100 μL of the pump contents could be pumped out during 4 wks, which represents 3.0×10^9 particles infused into the femoral medullary canal.

Reporter cells: RAW cells, and primary wild type and CCR2—macrophages

We used the differentiated murine macrophage cell line RAW 264.7³⁴ (a gift from Dr Gopalakrisman Sundaresan) transfected with the lentiviral vector to express the bioluminescent optical reporter gene firefly luciferase (*fluc*) and a fluorescence reporter gene green fluorescent protein (*gfp*). The cell line was grown in Dulbecco's Modified Eagle Medium 11995 (Gibco) + 10% fetal bovine serum. Each mouse received 0.5×10^6 cells suspended in 0.1 mL Hank's Balanced Salt Solution 14170 (Invitrogen, Carlsbad, CA) through a lateral tail vein injection (Day 0).

Macrophages were also harvested from femora of both CCR2^{-/-} and wild type C57BL mice. Cells were grown in Roswell Park Memorial Institute media (Gibco) + 10% horse serum; 5 ng/mL of M-CSF was added on the first day to differentiate bone marrow cells into macrophages. Then cells were transfected with the same lentiviral vector to express *fluc* and *gfp*. 5×10^6 wild type macrophages and CCR2^{-/-} macrophages were injected through the tail vein.

Imaging: microCT and bioluminescence (BLI)

A microCT scan was performed 1 day before surgery (day -8) and at day 20 for Groups 1 and 2 to detect changes in bone mineral density (BMD). At day 20, we euthanized the animals, then removed the implanted titanium rod from the distal femur to avoid metal artifact before microCT was performed. We used a phantom made of an epoxy-based resin that mimics hydroxyapatite and contains water and air inclusion for calibration. Anesthesia was maintained by mask inhalation of isoflurane, and animals were placed in the ventral position in the device (eXplore RS microCT, GE Medical, Raleigh, NC) with 49 μ m resolution during 8 mins. Irradiation was 19.2 Rads per mouse and per microCT. Before the procedure, scout images were made to confirm that both femurs were entirely scanned. After scanning, we used the scanner software for acquisition and scanner interface software for reconstruction. For BMD assessment we used MicroView software (GE Medical) and a 3D region of interest was created ($4 \times 3 \times 3$ mm) at the distal femur for each left femur.

For bioluminescence, we used an in vivo imaging system (IVIS) employing a cooled device camera (Caliper LifeScience, Hopkinton, MA). Animals were anesthetized with 3% isoflurane during the process. Bioluminescence was performed with 3mg/mouse of Luciferase substrate D-Luciferin (Biosynth Intl) administrated intraperitoneally. 5 mins later, images were taken of the whole mouse. We drew uniformly sized regions of interest (1.2×0.5 cm) at the level of the distal femur. Data were collected as to photon/sec/cm²/steradian (p/s/cm²/sr).

Histology and immunohistochemistry

After imaging, all animals were euthanized using both CO₂ inhalation and cervical dislocation. Femora were collected and decalcified using paraformaldehyde during 3 days and then ethylenediaminetetraacetic acid during 2 days twice. Frozen sections of 8 μ m were cut on a cryostat (Cambridge Instruments, Buffalo, NY) to include the distal third of the femora, where particles were infused. The sections collected were used for immunostaining. Rat anti-mouse macrophage/monocyte MOMA-2 (Abd Serotec, Raleigh, NC) was used to detect total macrophages. The secondary antibody used for immunofluorescence was goat anti-mouse/rabbit/rat IgG conjugated with Alexa Fluor 594 (Invitrogen, Carlsbad, CA). Using 20 \times magnification, we quantified the percentage of migrated reporter cells in the sections for Groups 1 and 2. 5 sections/group were randomly chosen for analysis. Within each section, the total number of cells (using DAPI staining) and reporter cells were counted, and the ratio expressed as a percentage. A reporter cell was defined as a cell having nuclear staining with DAPI and strong cytoplasmic signal with *gfp* when the images were overlaid. We also performed staining with hematoxylin and eosin (Sigma, Steinheim, Germany) on cut histological sections. Osteoclasts were identified using a leukocyte acid phosphatase kit, TRAP (Sigma).

Statistical analysis

Bioluminescence data (ratio of operated divided by non-operated femora), microCT data (BMD) and the quantified positive cells were analyzed by nonparametric Mann-Whitney U tests (two-tailed) between comparable paired groups (statistiXL software, Broadway-Nedlands, Australia).

RESULTS

Local injection of MCP-1 into the distal femoral canal induced systemic recruitment of intravenously injected RAW cell macrophages to the femur. This chemotactic effect was significantly higher than that seen with saline-injected controls on day 2 and day 4 (Fig. 3).

When RS102895, the CCR2B antagonist was injected, we observed a significant ($p = 0.009$) decrease of systemic migration of macrophages from day 8 to day 19. On day 19, the bioluminescence ratio was 0.91 ± 0.41 for Group 1 receiving the inhibitor and 3.58 ± 0.87 for Group 2 receiving control injections (Fig. 4). The same trends were observed using primary cells. From day 6 to 14, macrophage recruitment was significantly lower when CCR2-- reporter macrophages were infused compared to infusion of wild type reporter macrophages (Fig. 5). The bioluminescence ratio was 0.99 ± 0.52 for group 3 (CCR2-- reporter cell infusion) versus 1.26 ± 0.54 for group 4 ($p = 0.005$).

Histology and immunohistochemistry confirmed migration of reporter cells within the femoral shaft infused with particles (Fig. 6A–B). Osteoclast-like cells were more profuse for Group 2 vs. Group 1 (Fig 6C–D). Immunohistochemistry confirmed the results obtained by bioluminescence (Fig. 7): few reporter macrophages were found when MCP-1 receptor antagonist was given (Fig 7A). $5.5 \pm 2.2\%$ vs. $19.8 \pm 6.5\%$ ($p = 0.008$) of cells were migrated reporter cells for Groups 1 (with CCR2B inhibitor) and 2 (without inhibitor), respectively. The total number of cells was comparable in each image with no significant difference.

MicroCT analysis confirmed the protective effect of the MCP-1 receptor antagonist on particle-induced bone loss (Fig. 8). Total BMD was significantly decreased for Group 2 (Fig. 9B) (receiving particles but no antagonist) compared to Group 1 (receiving particles plus antagonist) at day 20 (Fig. 9A). After normalization (post minus pre values), BMD was 352.28 ± 36.65 for Group 1 versus 191.93 ± 41.34 for Group 2 ($p = 0.015$). BMD was similarly affected on the operated and non-operated sides of both groups, confirming the systemic effect of orthopaedic wear debris.

DISCUSSION

Given the fact that the most commonly used bearing surface for THA in the U.S. is metal-on-UHMWPE,³⁵ wear and the biological sequelae of wear debris are critical to implant longevity. UHMWPE particles stimulate a foreign body and chronic inflammatory reaction that can result in periprosthetic osteolysis, jeopardizing long-term implant stability.

Previously, it was assumed that the reaction to wear particles was a localized event. However recent studies demonstrated that UHMWPE wear particles stimulate systemic macrophage trafficking to the site of particle deposition. UHMWPE and metallic wear particles increase MCP-1 production in vitro.^{36,37} Furthermore, UHMWPE particle infusion stimulates macrophage recruitment in vivo and decreases BMD.³² However, the precise role that MCP-1 plays in systemic migration of macrophages in the presence of continuous particle infusion (similar to continuous particle production in humans) has not been elucidated.

Our current study provides strong experimental evidence of a relationship between the chemokine MCP-1 and systemic macrophage recruitment in the presence of UHMWPE particles. When the MCP-1 ligand-CCR2 receptor axis was interrupted by two interventions, macrophage trafficking was mitigated. Furthermore, disruption of the chemokine-receptor axis was associated with a decrease in the particle-associated adverse effects on BMD. Thus, modulation of this chemokine-receptor axis may provide a therapeutic strategy to diminish

particle-associated osteolysis. Ren et al also showed that macrophage depletion will ameliorate particle-associated osteolysis in a murine model.³⁸ However, this systemic effect, like systemic delivery of competitive inhibitors to MCP-1, compromises the important systemic immunomodulatory role of macrophages. Thus, local delivery strategies for decreasing particle-induced periprosthetic osteolysis seem more plausible.

Limitations to our study include the use of a murine model and the use of reporter RAW 264.7 cells that are an immortal macrophage cell line. These cells proliferate after migration and could increase bioluminescence within the region of interest; thus, increased bioluminescence reflects both systemic trafficking and proliferation of these cells at the local site. Furthermore, after about 2 to 3 wks, RAW cells may proliferate to the extent that they could induce cachexia of the mice. In consideration of these facts, we used primary wild type reporter macrophages that are not immortal cells to confirm the results obtained with RAW cells. Our results with primary cells confirm that the biological mechanisms associated with wear particle deposition are a systemic rather than a local phenomenon. The primary reporter cells were still able to migrate from the tail vein toward the site of particle infusion resulting in osteolysis.

Another interesting finding was the effects of some of the treatments on the contralateral femur. This phenomenon was seen in our previous study³² and has been noted with other animal models and clinical conditions.³⁹⁻⁴² The decrease of BMD of the non-operated femora might reflect systemic signaling induced by chronic inflammation. We also observed a similar effect of the MCP-1 antagonist for both operated and non-operated femur (Fig. 6) suggesting a systemic effect. Indeed, Gong et al.⁴³ showed a systemic effect of the MCP-1 antagonist, decreasing bone destruction in a mouse model of systemic arthritis.⁴⁴ Binder et al. also demonstrated this systemic effect on bone mass using CCR2 $-/-$ and MCP-1 deficient mice.⁴⁵

Bar-Shira-Maymon et al. showed that BMD of mice increase up to 13.5 mos of age in vertebra.⁴⁶ Beamer et al. showed that adult peak BMD was typically achieved by 4 mos of age for the mouse femur.⁴⁷ Our mice were 3 mos of age prior to euthanasia. A similar study as our current one using older mice would confirm the preventive role of a CCR2 receptor antagonist in the physiological condition of osteopenia.

In conclusion, MCP-1 is a key chemokine that modulates macrophage recruitment. Using a clinically relevant murine model of continuous local UHMWPE wear particle infusion, our hypothesis was confirmed: we demonstrated that disruption of the MCP-1 ligand-CCR2 receptor axis can mitigate systemic macrophage recruitment and particle-associated bone loss. Modulation of this chemokine-receptor axis may provide a therapeutic strategy to diminish particle-associated periprosthetic osteolysis.

Acknowledgments

We thank Dr Gobalakrisman Sundaresan who supplied the Fluc and GFP expressing RAW Cells 264.7 macrophage cell line and Timothy Wright PhD who supplied the UHMWPE particles. This research was supported by NIH (Grant 1R01AR055650-04).

REFERENCES

1. Sundfeldt M, Carlsson LV, Johansson CB, et al. Aseptic loosening, not only a question of wear: a review of different theories. *Acta Orthop.* 2006; 77:177-197. [PubMed: 16752278]
2. Kurtz S, Ong K, Lau E, et al. Projections of primary and revision hip and knee arthroplasty in the United States from 2005 to 2030. *J Bone Joint Surg Am.* 2007; 89:780-785. [PubMed: 17403800]

3. Goodman SB, Huie P, Song Y, et al. Cellular profile and cytokine production at prosthetic interfaces. Study of tissues retrieved from revised hip and knee replacements. *J Bone Joint Surg Br.* 1998; 80:531–539. [PubMed: 9619952]
4. Kadoya Y, Revell PA, al-Saffar N, et al. Bone formation and bone resorption in failed total joint arthroplasties: histomorphometric analysis with histochemical and immunohistochemical technique. *J Orthop Res.* 1996; 14:473–482. [PubMed: 8676261]
5. Bostrom M, O’Keefe R. What experimental approaches (eg, in vivo, in vitro, tissue retrieval) are effective in investigating the biologic effects of particles? *J Am Acad Orthop Surg.* 2008; 16 Suppl 1:S63–S67. [PubMed: 18612016]
6. Wang ML, Sharkey PF, Tuan RS. Particle bioreactivity and wear-mediated osteolysis. *J Arthroplasty.* 2004; 19:1028–1038. [PubMed: 15586339]
7. Schmalzried TP, Jasty M, Harris WH. Periprosthetic bone loss in total hip arthroplasty. Polyethylene wear debris and the concept of the effective joint space. *J Bone Joint Surg Am.* 1992; 74:849–863. [PubMed: 1634575]
8. Shanbhag AS, Jacobs JJ, Glant TT, et al. Composition and morphology of wear debris in failed uncemented total hip replacement. *J Bone Joint Surg Br.* 1994; 76:60–67. [PubMed: 8300684]
9. Doorn PF, Campbell PA, Worrall J, et al. Metal wear particle characterization from metal on metal total hip replacements: transmission electron microscopy study of periprosthetic tissues and isolated particles. *J Biomed Mater Res.* 1998; 42:103–111. [PubMed: 9740012]
10. Goodman SB. Wear particles, periprosthetic osteolysis and the immune system. *Biomaterials.* 2007; 28:5044–5048. [PubMed: 17645943]
11. Ren PG, Huang Z, Ma T, et al. Surveillance of systemic trafficking of macrophages induced by UHMWPE particles in nude mice by noninvasive imaging. *J Biomed Mater Res A.* 2010; 94:706–711. [PubMed: 20213815]
12. Goodman SB, Ma T. Cellular chemotaxis induced by wear particles from joint replacements. *Biomaterials.* 2010; 31:5045–5050. [PubMed: 20398931]
13. Endres S, Bartsch I, Sturz S, et al. Polyethylene and cobalt-chromium molybdenum particles elicit a different immune response in vitro. *J Mater Sci Mater Med.* 2008; 19:1209–1214. [PubMed: 17701308]
14. Epstein NJ, Bragg WE, Ma T, et al. UHMWPE wear debris upregulates mononuclear cell proinflammatory gene expression in a novel murine model of intramedullary particle disease. *Acta Orthop.* 2005; 76:412–420. [PubMed: 16156472]
15. Ren W, Wu B, Mayton L, Wooley PH. Polyethylene and methyl methacrylate particle-stimulated inflammatory tissue and macrophages up-regulate bone resorption in a murine neonatal calvaria in vitro organ system. *J Orthop Res.* 2002; 20:1031–1037. [PubMed: 12382970]
16. Athanasou NA, Quinn J, Bulstrode CJ. Resorption of bone by inflammatory cells derived from the joint capsule of hip arthroplasties. *J Bone Joint Surg Br.* 1992; 74:57–62. [PubMed: 1732267]
17. Sabokbar A, Pandey R, Quinn JM, Athanasou NA. Osteoclastic differentiation by mononuclear phagocytes containing biomaterial particles. *Arch Orthop Trauma Surg.* 1998; 117:136–140. [PubMed: 9521517]
18. Bauer TW. Particles and periimplant bone resorption. *Clin Orthop Relat Res.* 2002:138–143. [PubMed: 12461365]
19. Tuan RS, Lee FY, Y TK, et al. What are the local and systemic biologic reactions and mediators to wear debris, and what host factors determine or modulate the biologic response to wear particles? *J Am Acad Orthop Surg.* 2008; 16 Suppl 1:S42–S48. [PubMed: 18612013]
20. Goodman SB, Trindade M, Ma T, et al. Pharmacologic modulation of periprosthetic osteolysis. *Clin Orthop Relat Res.* 2005:39–45. [PubMed: 15662302]
21. Deshmane SL, Kremlev S, Amini S, Sawaya BE. Monocyte chemoattractant protein-1 (MCP-1): an overview. *J Interferon Cytokine Res.* 2009; 29:313–326. [PubMed: 19441883]
22. Fritz EA, Glant TT, Vermes C, et al. Titanium particles induce the immediate early stress responsive chemokines IL-8 and MCP-1 in osteoblasts. *J Orthop Res.* 2002; 20:490–498. [PubMed: 12038622]
23. Trindade MC, Schurman DJ, Maloney WJ, et al. G-protein activity requirement for polymethylmethacrylate and titanium particle-induced fibroblast interleukin-6 and monocyte

- chemoattractant protein-1 release in vitro. *J Biomed Mater Res*. 2000; 51:360–368. [PubMed: 10880077]
24. Huang Z, Ma T, Ren PG, et al. Effects of orthopedic polymer particles on chemotaxis of macrophages and mesenchymal stem cells. *J Biomed Mater Res A*. 2010; 94:1264–1269. [PubMed: 20694994]
 25. Glant TT, Jacobs JJ, Molnar G, et al. Bone resorption activity of particulate-stimulated macrophages. *J Bone Miner Res*. 1993; 8:1071–1079. [PubMed: 8237476]
 26. Green TR, Fisher J, Matthews JB, et al. Effect of size and dose on bone resorption activity of macrophages by in vitro clinically relevant ultra high molecular weight polyethylene particles. *J Biomed Mater Res*. 2000; 53:490–497. [PubMed: 10984696]
 27. Horowitz SM, Gonzales JB. Effects of polyethylene on macrophages. *J Orthop Res*. 1997; 15:50–56. [PubMed: 9066526]
 28. Kim KJ, Kobayashi Y, Itoh T. Osteolysis model with continuous infusion of polyethylene particles. *Clin Orthop Relat Res*. 1998:46–52. [PubMed: 9678032]
 29. Ma T, Huang Z, Ren PG, et al. An in vivo murine model of continuous intramedullary infusion of polyethylene particles. *Biomaterials*. 2008; 29:3738–3742. [PubMed: 18561997]
 30. Ortiz SG, Ma T, Regula D, et al. Continuous intramedullary polymer particle infusion using a murine femoral explant model. *J Biomed Mater Res B Appl Biomater*. 2008; 87:440–446. [PubMed: 18536041]
 31. von Knoch M, Jewison DE, Sibonga JD, et al. The effectiveness of polyethylene versus titanium particles in inducing osteolysis in vivo. *J Orthop Res*. 2004; 22:237–243. [PubMed: 15013080]
 32. Ren PG, Irani A, Huang Z, et al. Continuous Infusion of UHMWPE Particles Induces Increased Bone Macrophages and Osteolysis. *Clin Orthop Relat Res*. 2011; 469:113–122. [PubMed: 21042895]
 33. Campbell P, Ma S, Yeom B, et al. Isolation of predominantly submicron-sized UHMWPE wear particles from periprosthetic tissues. *J Biomed Mater Res*. 1995; 29:127–131. [PubMed: 7713952]
 34. Raschke WC, Baird S, Ralph P, Nakoinz I. Functional macrophage cell lines transformed by Abelson leukemia virus. *Cell*. 1978; 15:261–267. [PubMed: 212198]
 35. Bozic KJ, Kurtz S, Lau E, et al. The epidemiology of bearing surface usage in total hip arthroplasty in the United States. *J Bone Joint Surg Am*. 2009; 91:1614–1620. [PubMed: 19571083]
 36. Nakashima Y, Sun DH, Trindade MC, et al. Induction of macrophage C-C chemokine expression by titanium alloy and bone cement particles. *J Bone Joint Surg Br*. 1999; 81:155–162. [PubMed: 10068024]
 37. Yaszay B, Trindade MC, Lind M, et al. Fibroblast expression of C-C chemokines in response to orthopaedic biomaterial particle challenge in vitro. *J Orthop Res*. 2001; 19:970–976. [PubMed: 11562149]
 38. Ren W, Markel DC, Schwendener R, et al. Macrophage depletion diminishes implant-wear-induced inflammatory osteolysis in a mouse model. *J Biomed Mater Res A*. 2008; 85:1043–1051. [PubMed: 17937417]
 39. Decaris E, Guingamp C, Chat M, et al. Evidence for neurogenic transmission inducing degenerative cartilage damage distant from local inflammation. *Arthritis and Rheumatism*. 1999; 42:1951–1960. [PubMed: 10513812]
 40. Donaldson LF, Seckl JR, McQueen DS. A discrete adjuvant-induced monoarthritis in the rat: effects of adjuvant dose. *Journal of Neuroscience Methods*. 1993; 49:5–10. [PubMed: 8271831]
 41. Kelly S, Dunham JP, Donaldson LF. Sensory nerves have altered function contralateral to a monoarthritis and may contribute to the symmetrical spread of inflammation. *The European Journal of Neuroscience*. 2007; 26:935–942. [PubMed: 17714187]
 42. Kumagai K, Vasanji A, Drazba JA, et al. Circulating cells with osteogenic potential are physiologically mobilized into the fracture healing site in the parabiotic mice model. *J Orthop Res*. 2008; 26:165–175. [PubMed: 17729300]
 43. Gong JH, Ratkay LG, Waterfield JD, Clark-Lewis I. An antagonist of monocyte chemoattractant protein 1 (MCP-1) inhibits arthritis in the MRL-lpr mouse model. *The Journal of Experimental Medicine*. 1997; 186:131–137. [PubMed: 9207007]

44. Ratkay LG, Zhang L, Tonzetich J, Waterfield JD. Complete Freund's adjuvant induces an earlier and more severe arthritis in MRL-lpr mice. *Journal of Immunology* (Baltimore, Md.: 1950). 1993; 151:5081–5087.
45. Binder NB, Niederreiter B, Hoffmann O, et al. Estrogen-dependent and C-C chemokine receptor-2-dependent pathways determine osteoclast behavior in osteoporosis. *Nature Medicine*. 2009; 15:417–424.
46. Bar-Shira-Maymon B, Coleman R, Cohen A, et al. Age-related bone loss in lumbar vertebrae of CW-1 female mice: a histomorphometric study. *Calcif Tissue Int*. 1989; 44:36–45. [PubMed: 2492885]
47. Beamer WG, Donahue LR, Rosen CJ, Baylink DJ. Genetic variability in adult bone density among inbred strains of mice. *Bone*. 1996; 18:397–403. [PubMed: 8739896]

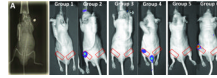


Figure 1. Image of the infusion pump set-up (A) and bioluminescence pictures of each condition at critical time points: at day 10 for Groups 1 and 2, day 8 for Groups 3 and 4, day 4 for Groups 5 and 6. Red rectangles indicate the region of interest for bioluminescence analysis.

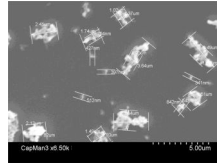


Figure 2.
SEM photomicrograph of UHMWPE particles.

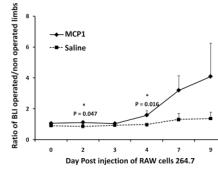


Figure 3.

Graph showing the effect of MCP-1 on systemic macrophage migration. At day 4, the ratio of BLI (treatment side divided by the contralateral side) was 0.98 ± 0.10 for Group 5 (the saline injected group) and 1.58 ± 0.31 in Group 6 receiving the MCP-1 injection.

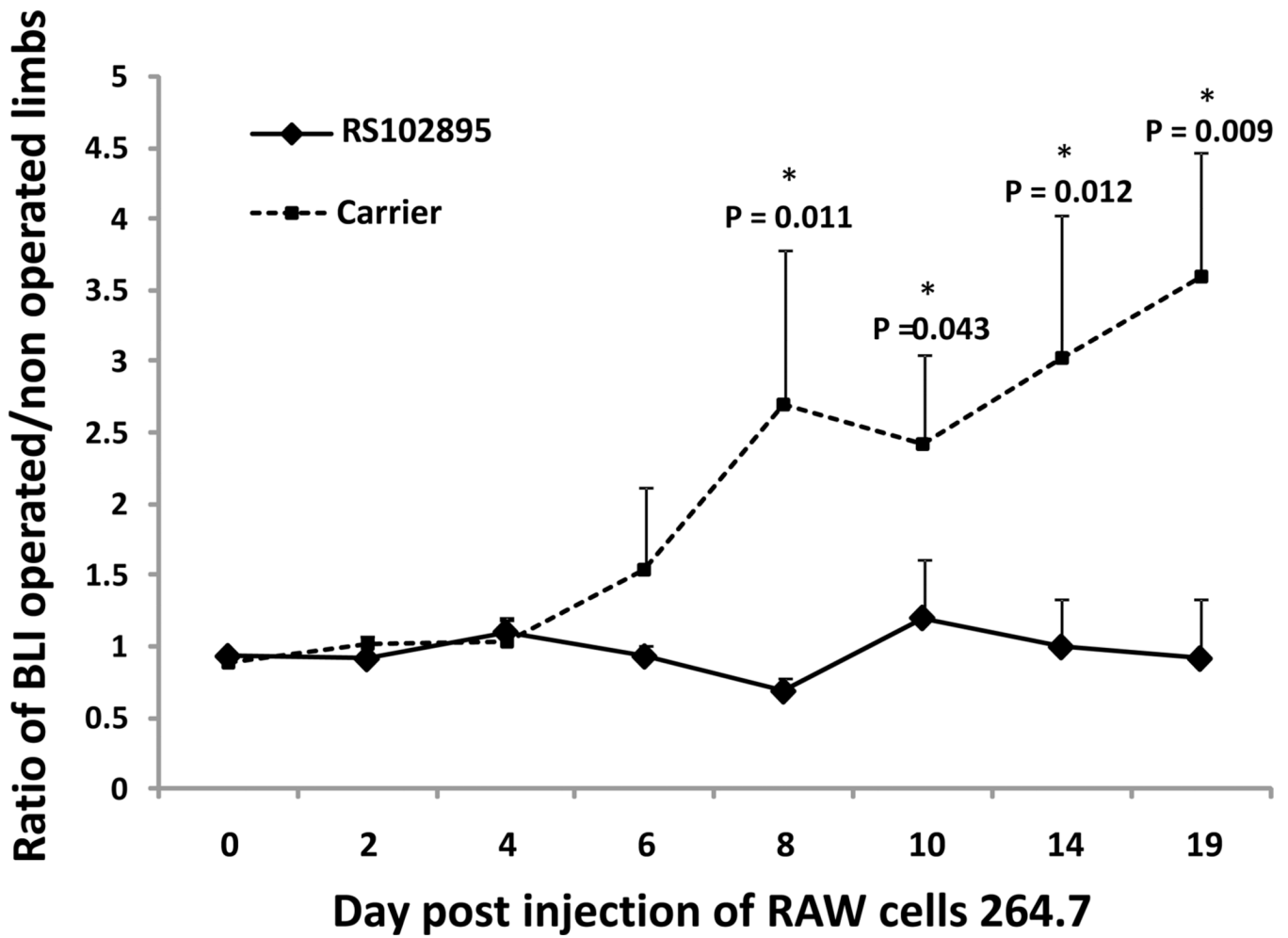


Figure 4. Ratio of bioluminescence signal from operated (infusion of UHMWPE particles) femora divided by the corresponding non-operated contralateral femora from Day 0 to 19 post reporter cell injection using RAW cells. The ratio was significantly lower when the MCP-1 receptor antagonist (RS102895) was given.

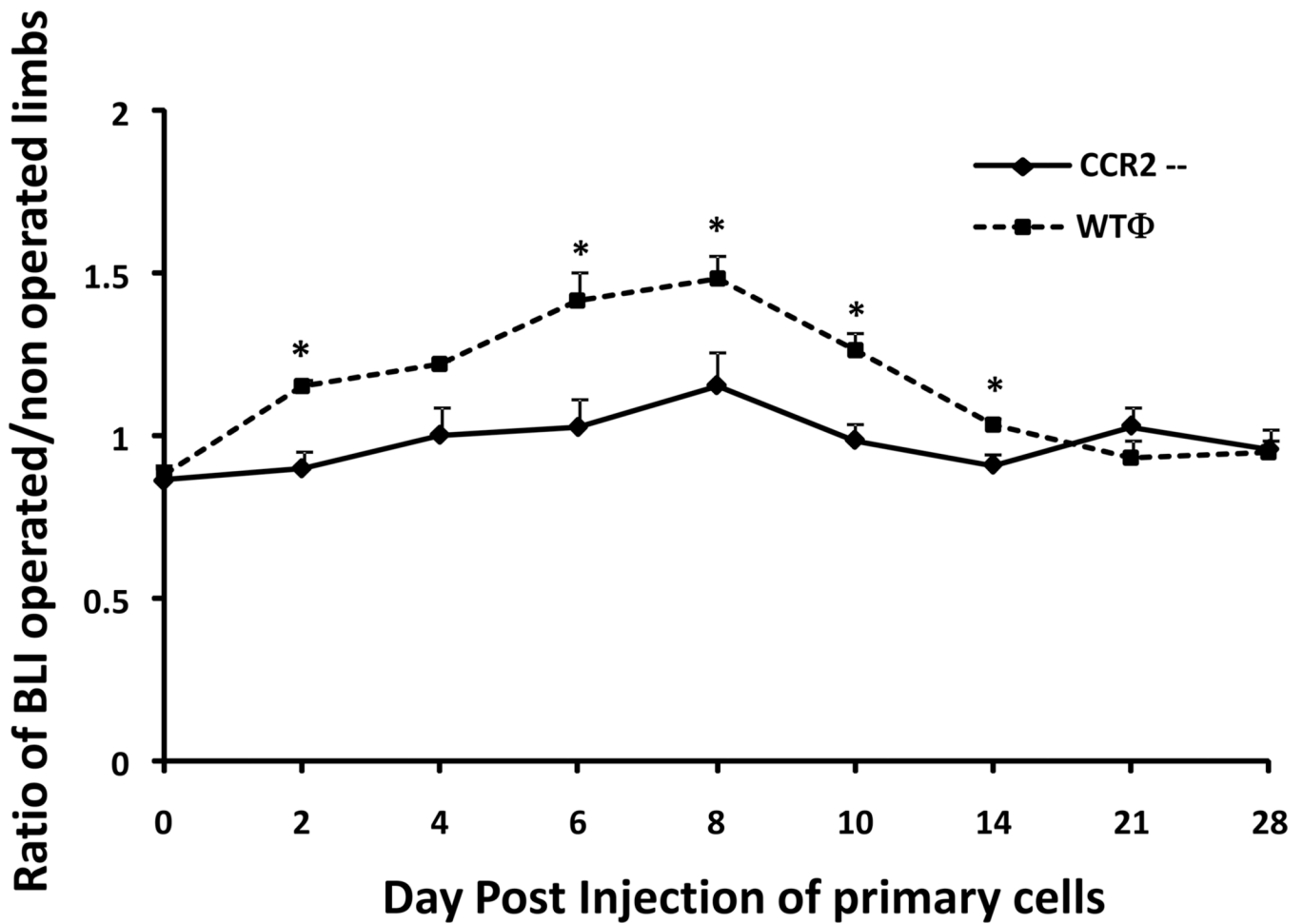


Figure 5.

Chemotaxis of primary murine macrophages in the presence of UHWMPE. Primary cells were injected through the tail vein. Systemic migration macrophages were significantly lower when macrophages deficient in the CCR2 receptor were injected. CCR2^{-/-} = macrophages deficient in the CCR2 receptor; WTΦ = wild type macrophages. * = $p < 0.005$.

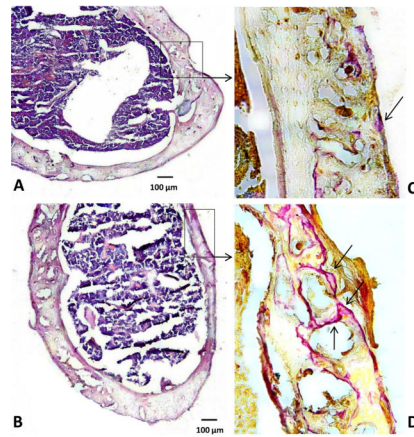


Figure 6. Hematoxylin and eosin (A–B) and TRAP staining for osteoclast-like cells (C–D) from Group 1 (A–C) and Group 2 (B–D). Few osteoclasts (arrows) were observed for Group 1 (with particle infusion and inhibitor) versus Group 2 (with particle infusion only). (H&E original magnification = 10 \times ; TRAP, original magnification = 20 \times)

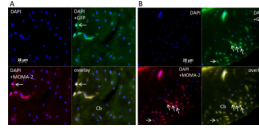


Figure 7. Immunohistochemistry for Group 1 (A) and Group 2 (B). Reporter macrophages containing GFP (green), total macrophages stained with MOMA-2 (red), overlay of GFP and MOMA-2 images showing migrated reporter macrophages (yellow). Few reporter macrophages (arrows) were observed when MCP-1 receptor antagonist was injected. Cb = cortical bone. (original magnification = 20 \times).

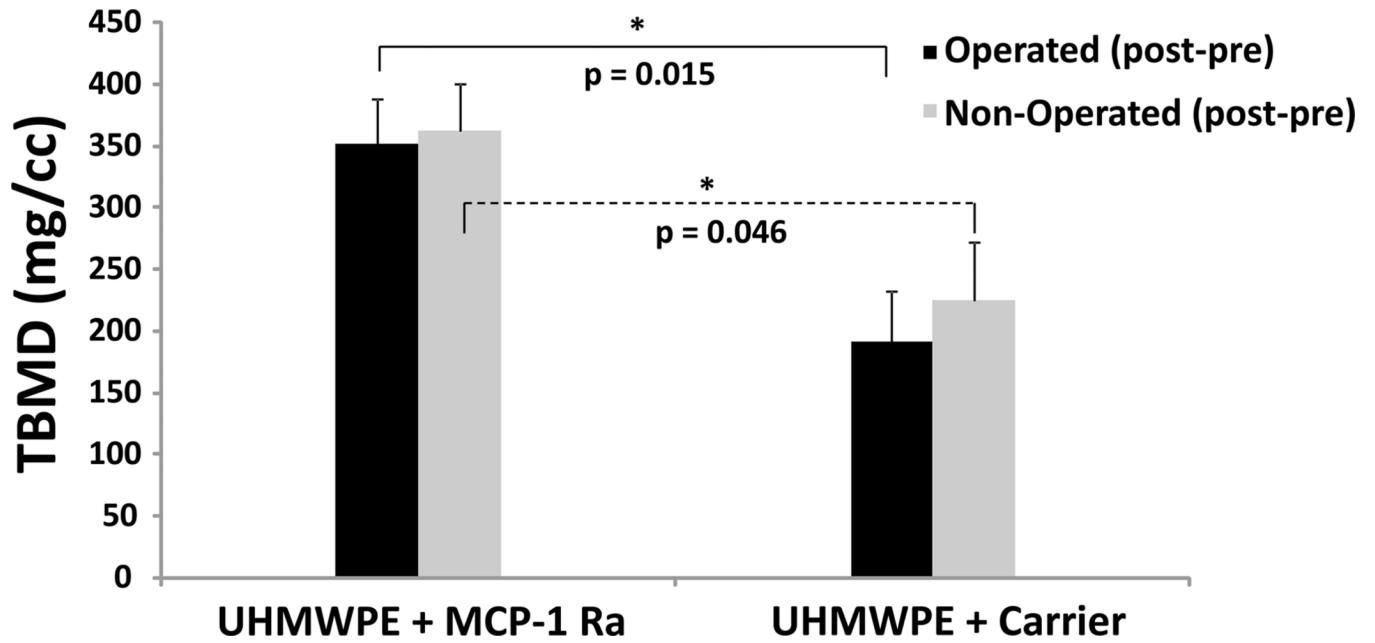


Figure 8. Bone loss (decreased BMD) was significantly lower when mice were treated with MCP-1 receptor antagonist (MCP-1 Ra) compared to controls. TBMD = total bone mineral density.

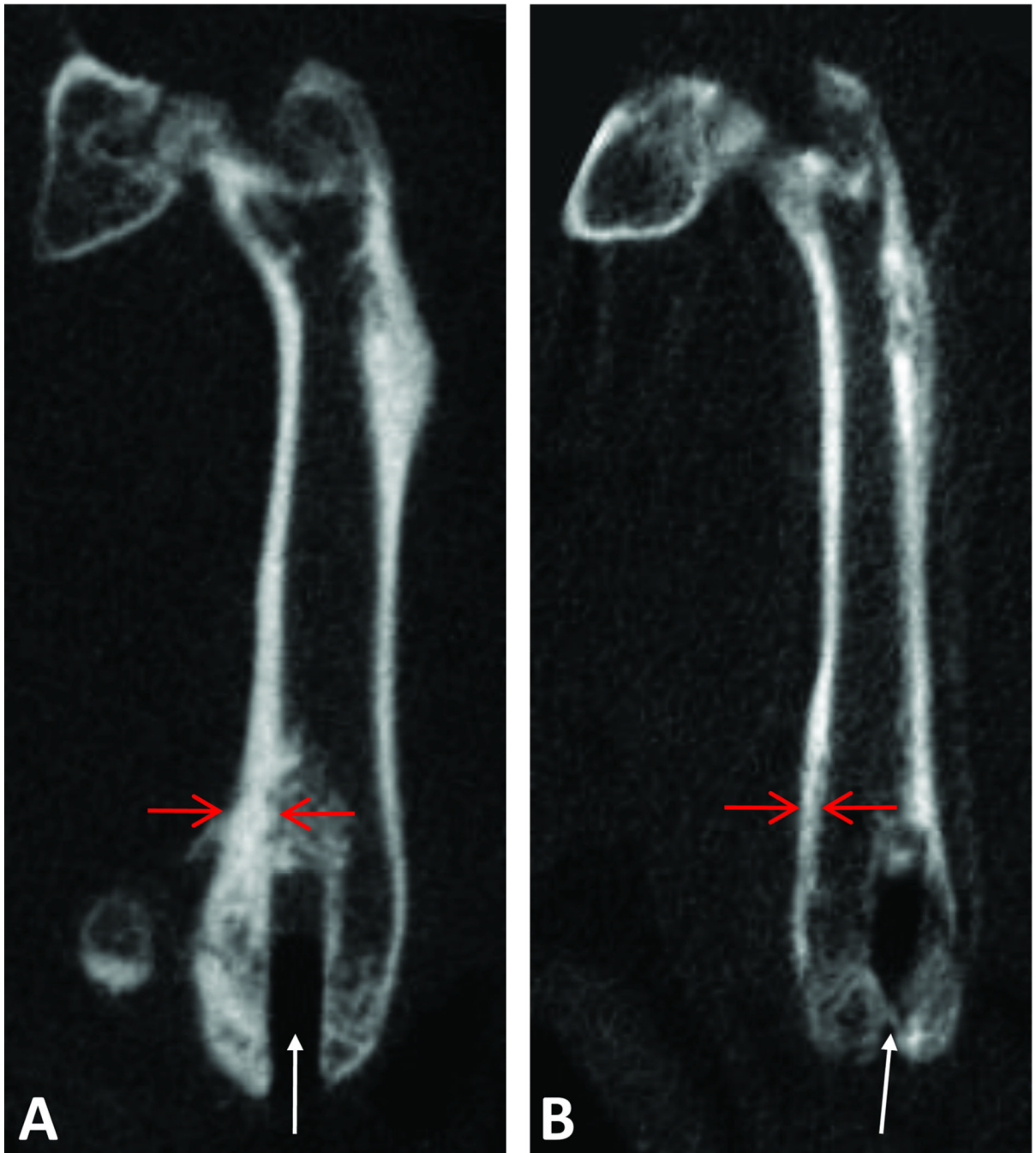


Figure 9. MicroCT reconstruction images of operated femur from Group 1 (A) and Group 2 (B). The footprint of the Ti rod is visible (white arrows). The cortical bone (red arrows) appears thicker when the MCP-1 receptor antagonist (Group 1) was given.

Table 1

Experimental design. MCP-1 Ra = MCP-1 Receptor antagonist given twice per week by intraperitoneal injection; MCP-1 = a single intramedullary injection of MCP-1; RAW = RAW 264.7 macrophage cell line; CCR2-- = macrophages deficient in the CCR2 receptor; WT Φ = wild type macrophages.

	n	UHMWPE in pump	MCP-1 Ra	MCP-1	Carrier	Cells Injected Via Tail Vein
Group 1	10	✓	✓			RAW
Group 2	10	✓			✓	RAW
Group 3	9	✓				CCR2--
Group 4	7	✓				WT Φ
Group 5	8				✓	RAW
Group 6	12			✓		RAW